ECS Transactions, 61 (11) 25-40 (2014)
10.1149/06111.0025ecst ©The Electrochemical Society

On the electrochemical deposition of Metal-Organic Frameworks

N. Campagnol[a], T. R. C. Van Assche[b], L. Stappers[a],
J. F. M. Denayer[b], K. Binnemans[c], D. E. De Vos[d], and J. Fransaer[a]

[a] Department of Materials Engineering (MTM), KU Leuven,
Kasteelpark Arenberg 44, B-3001 Leuven, Belgium
[b] Department of Chemical Engineering, Vrije Universiteit Brussel,
Pleinlaan 2, B-1050 Brussels, Belgium
[c] Centre for Surface Chemistry and Catalysis (COK), KU Leuven,
Kasteelpark Arenberg 23, B-3001 Leuven, Belgium
[d] Department of Chemistry, KU Leuven,
Celestijnenlaan 200F, B-3001 Leuven, Belgium

The electrochemical deposition of Metal-Organic Frameworks (MOFs) is an interesting technique to synthesize adherent, microporous layers on top of metal substrates. However, up to now not much is known about this process, and in this paper a four phase mechanism is proposed to better understand it. The study focuses on how the nucleation of these compounds starts and proceeds, what the influence of the solvent is, the stresses in the growing layers, and the origin of defects like delamination and crystal detachment.

Introduction

Metal-Organic Frameworks (MOFs) are a novel class of materials with very high porosity. These compounds are based on metal (or metal-oxygen) centers, connected by organic linkers to form light and hollow 1D, 2D or 3D structures.[1, 2] The choice of many possible metals and a virtually infinite number of linkers, make them extremely tunable and adjustable for different applications.[3]

MOF structures are obtained by self-assembly of the organic linkers with the metal ions, typically supplied in a solvent as a weak organic acid and a metal salt, respectively. A new method patented by BASF proposes to deliver the ions electrochemically by anodic dissolution, avoiding the use of salts and reducing the synthesis time.[4] Later, Ameloot *et al.* reported that this technique can be used to electrodeposit MOF coatings if the formed coordination polymers assemble on the anodic surface.[5] The synthesis of MOF films is very important for a wide range of applications,[6] and in particular electrochemically synthesized MOF layers have been successfully tested for humidity,[3] oxygen and glucose sensing,[7] gas separation,[8, 9] and membranes.[10] As shown in recent publications, these layers are compact and well adherent,[11] and if synthesized under certain conditions, they can be more than one crystal layer thick.[8] Still, several questions about the deposition mechanism remain unresolved. For example some researchers claim the possibility to electrochemically synthesize important MOFs like the Zn-methylimidazolate ZIF-8 in the form of powders, but the impossibility to make layers.[12] Moreover, in order to grow thick MOF layers it is important to know where the crystals grow when a closed layer has been formed already, either at the bottom or at the top of the already formed ones. This has

implications on the adhesion of the layers, because if the layers grow at the MOF-solution interface, the adhesion between the MOF layer and the substrate will eventually be lost as the MOF layer gets undercut by the dissolution of the substrate. Another possible occurrence is that a different phase without linker, like an oxide or hydroxide, might form at the MOF-substrate interface, equally undermining the layer adhesion. In fact, defects of the MOF layers synthesized with the electrochemical technique have already been reported, but the origin of this phenomenon has not yet been explained.[9]
In this paper, the electrochemical nucleation and growth of MOF layers are shown to proceed in four phases. Information about these four phases was obtained using different experimental techniques, *i.e.* Electrochemical Quartz Crystal Microbalance (EQCM), a homemade laser curvature setup, and Scanning Electron Microscopy (SEM) equipped with Energy Dispersion Spectroscopy (EDS). Most of the information was obtained with the electrochemically grown archetypical MOF HKUST-1 (Cu-BTC, based on copper and trimesic acid or H_3BTC), but for some specific experiments substituted versions of copper isonicotinate (Cu-INA) with chlorine or fluorine atoms in position 2 of the linker ring were used.

Experimental

Synthesis of HKUST-1

To study the influence of the solvent and the variation in crystals dimensions, HKUST-1 was synthesized electrochemically on thin copper meshes (99.98% copper, 8 µm thick with windows of *ca* 50 μm^2,by Precision Eforming, U.S.A.). Methanol (MeOH, Sigma Aldrich, 99.8%), ethanol (EtOH, VWR, 99.9%), N,N-dimethylformamide (DMF, Sigma Aldrich, 99.8%), dimethylsulfoxide (DMSO, Sigma Aldrich, 99.9%) and acetonitrile (ACN, Sigma Aldrich, 99.8%) were used as solvents, typically with water as cosolvent. The linker for these synthesis mixtures was 1,3,5-benzenetricarboxylic acid (trimesic acid, H_3BTC, Sigma Aldrich, 95%) in a concentration of 16 g/L. Other synthesis details are reported in a recent paper.[10]
To study the four phases of the electrodeposition, the same MOF was synthesized using copper-coated silicon wafers or platinum-coated quartz crystals (Testbourne, area 1.37 cm^2) as working electrodes. For the Electrochemical Quartz Crystal Microbalance (EQCM) experiments the platinum-coated faces of the vibrating crystals were first electroplated with copper. The electrochemical experiments were controlled by a galvanostat/potentiostat (EG&G, model 273 or Solartron SI 1287) and an EQCM apparatus (RQCM, Inficon). A 2 cm thick mask was placed in front of the working electrode to prevent edge effects.[13] A home-made Ag/AgCl (3 M KCl) served as reference, and platinum foils (with different dimensions depending on the experiment but always larger than the surface of the working electrode) were used as counter electrode. Except where stated otherwise, the solution consists of EtOH/water (67:33 vol%) with 10 g/L of H_3BTC.[8]
In-situ stress measurements during MOF films growth were performed using a home-built laser curvature setup.[14] The setup consists of a red laser (R-30995, Newport) which is focused on a glass cantilever (D 263 Schott, 60 x 3 x 0.108 mm) coated with 250 nm of gold on one side. When stressed films are deposited on the gold-plated face, the cantilever bends and the laser beam is deflected. Laser beam deflection is measured using a duo-lateral Position Sensitive Device (PSD, DLS-20 by UTD Sensors Inc). The relation

between the laser deflection and the force per unit width *F/w* is given by Stoney's formula:

$$\frac{F}{w} = \frac{Et^2 n_{air} d}{12(1-\nu)Ln_{ethanol}D}$$

where *E*, ν and *t* are Young's modulus, Poisson ratio and thickness of the cantilever. The length of the unclamped part of the cantilever is *L*, *n* is the refractive index of ethanol or air, *D* is the distance between the cantilever and the PSD, and *d* is the deflection of the laser beam at the PSD.

To determine stresses in MOF films, first a 2 μm layer of copper was electrodeposited on the cantilever's gold-coated face causing tensile stress to arise. As a blank, thin film stress was measured during dissolution of copper in an EtOH/water (67:33 vol%) electrolyte without H_3BTC but with 10 g/L methyltributylammonium methyl sulfate (MTBS, Sigma-Aldrich, 95%) to enhance the conductivity. The same experiment was repeated with the same electrolyte with 10 g/L of H_3BTC and 10 g/L of MTBS.

Synthesis of Cu-INA, Cu-INA(Cl) and Cu-INA(F)

A different system, Cu-INA, was used to compare the results obtained with HKUST-1. The electrolytes used for the synthesis are the following: 5.8 mmol of ligand (714 mg isonicotinic acid (HINA), or 818 mg of HINA(F) or 914 mg of HINA(Cl)), 1 g of MTBS in 100 mL of H_2O/EtOH (50:50 vol%). 2-chloropyridine-4-carboxylic acid (INA(Cl) 98%) and 2-fluoropyridine-4-carboxylic acid (INA(F) 98%) were purchased from Matrix Scientific, while the pyridine-4-carboxylic acid (HINA, 99%) used is produced by Sigma-Aldrich.

The depositions were run in a small two electrodes set-up with different applied potentials vs the counter electrode (a platinum coil), for different durations, and always at 60 °C. Cu-INA was deposited at 3 V for 3 min, Cu-INA(Cl) for 4 min at 2 V, and Cu-INA(F) at 3 V for 4 min. The substrates used are copper plates with a surface of *circa* 1-2 cm^2. The electrolyte mix is not soluble at room temperature and has therefore to be stirred at 60 °C for several minutes before a clear solution is obtained. Very important for the synthesis is to avoid dipping the copper plates in solution before the desired temperature is reached, since contact of the copper surfaces with the electrolyte starts the reaction, but leads to undesired phases.

Adsorption of m-xylene and TIPB

3.0 wt% m-xylene (>98%, Fluka) and 3.2 wt% 1,3,5-tris(propan-2-yl)benzene (>95%; Fluka) in isooctane (>99%, Biosolve) mixtures were prepared and added to activated (8 h, 180 °C) Cu-BTC. Three vials of each liquid were prepared, stored at 6 °C and sampled (at 6 °C) after respectively 1, 4 and 16 days. The samples were analyzed using a GC-FID method.

Characterization

Scanning electron microscopy (SEM) and energy dispersive spectroscopy (EDS) were done with a JEOL 6400, a FEI XL30, or a FEI-Nova NanoSEM 450. As MOFs are not

conductive, the samples were sputtered before SEM observation with Pt/Pd in order to increase the conductivity and improve the imaging. X-ray diffraction patterns were recorded with a Seifert 3003 T. Gas sorption measurements were run with a VTI SGA-100H gravimetric uptake device. On all the HKUST-1 meshes (synthesized with different synthesis mixtures), methanol vapor adsorption at 323 K was performed using a SGA-100H (VTI corporation) gravimetric uptake device.

Results and discussion

According to our proposed model, the deposition of MOFs happens in four phases: (I) initial nucleation, (II) island growth, (III) intergrowth and (IIII) detachment, schematically shown in Figure 1 and represented in the SEM pictures of Figure 2.

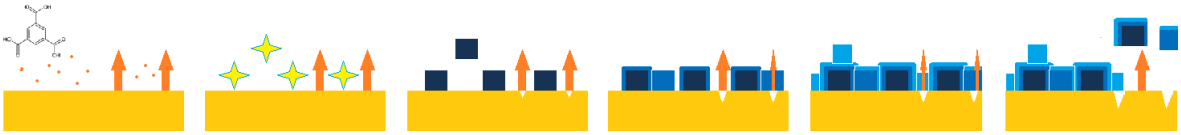

Figure 1: Proposed mechanism of MOF electrodeposition: copper(II) ions are released in solution where the linker is present; when the critical concentration of reagents is reached nuclei form in solution and on the surface (Phase I: Initial nucleation); these nuclei grow to micrometric-sized crystals on the surface next to and on top of each other (Phase II: Growth of islands); new crystals keep on nucleating (progressive nucleation) and grow forming an intergrown layer (Phase III: Intergrowth), and lastly parts of the MOF layer lose contact with the substrate and are released into the solution, probably aided by the internal stress in the MOF layer (Phase IIII: Detachment).

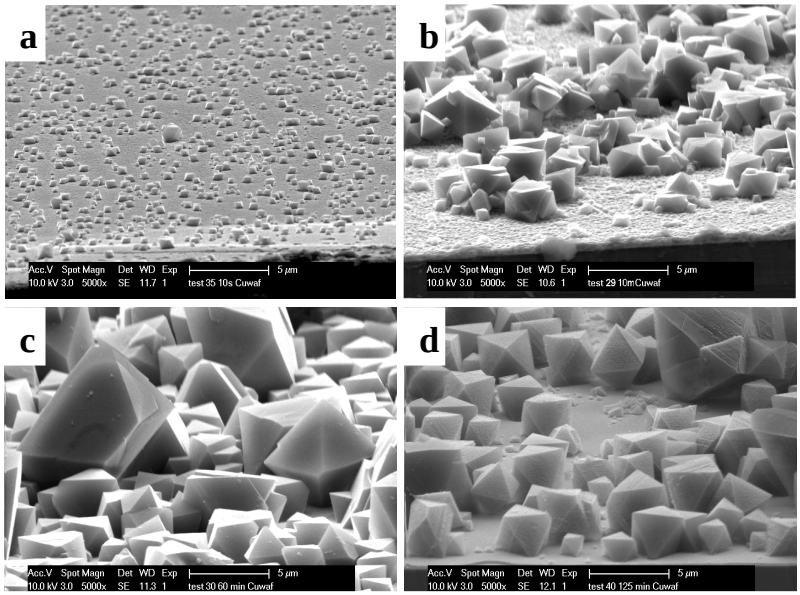

Figure 2: SEM pictures taken at a 75° angle with the normal of the four phases. Initial nucleation (a), growth of islands (b), intergrowth (c) and detachment (d). Copper-coated wafer substrate, 2 V vs counter electrode, after 10 s, 10 min, 60 min and 125 min.

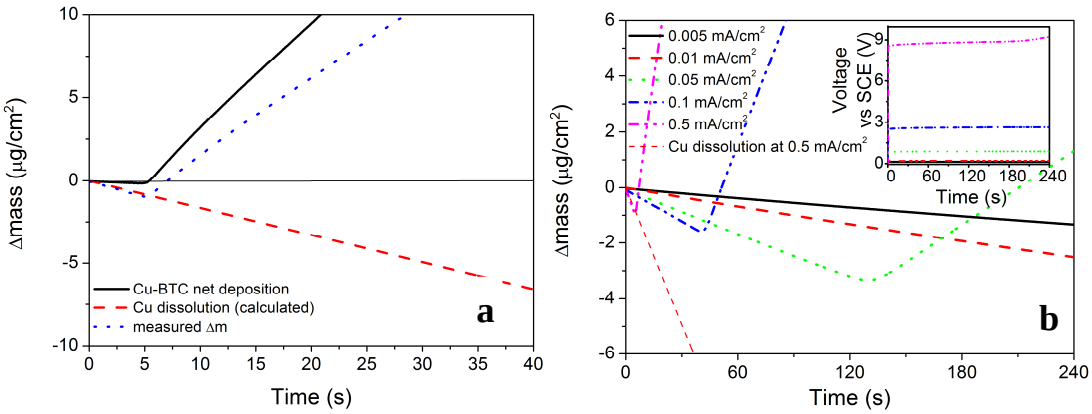

Figure 3: (a) EQCM plot with the measured mass variation, the calculated loss in mass assuming 100% efficiency of Cu dissolution, and the net deposition of MOF (experiment run at 0.5 mA/cm^2). (b) EQCM plots of HKUST-1 deposition at different current densities (the inset shows the potential during deposition).

Phase 1: initial nucleation

During the initial nucleation, the metal substrate starts dissolving anodically in the solution containing the linker, and the first crystals nucleate on the electrode surface. The nucleation tends to start from defects of the substrate, but if a very flat surface (e.g. a wafer) is used, isolated nearly monodisperse crystals can be observed after nucleation (Figure 2a).

The nucleation phase was studied with an EQCM (Figure 3). During the galvanic deposition of HKUST-1 it is observed that nucleation happens only after a lag time during which the mass of the electrode decreases (Figure 3a). This effect can be explained by the fact that a critical metal ion concentration (C_c) needs to be reached above the electrode surface to start the nucleation of the new MOF phase. When the critical concentration is reached, the EQCM signal bends upward, corresponding to a net increase in the mass of the vibrating quartz crystal. A similar effect was reported earlier for phosphate conversion layers,[15] and the event can be isolated by subtracting the variation of mass due to the copper dissolution (calculated using Faraday's law and assuming 100% current efficiency for the dissolution of copper), from the variation of mass measured at the electrode (Figure 3a).

Figure 3b shows EQCM plots taken during electrochemical depositions done at different current densities. It is evident that more time and more metal ions are needed to start the deposition if lower currents are used. At the lowest current densities the nucleation threshold is never reached and the only thing that happens is the dissolution of the copper layer in the solution, and therefore the formation of MOF crystals as precipitate and not as a coating.

After the first MOF crystals have nucleated, the deposition can proceed without the need for new nucleation. This is illustrated in Figure 4 where a galvanostatic deposition of HKUST-1 at 0.1 mA/cm^2 was split in two parts separated by a period of 10 min during which no current was applied. During this interruption, the reactants created or accumulated at the surface during the first deposition step can diffuse in the solution, restoring the pre-synthesis conditions.

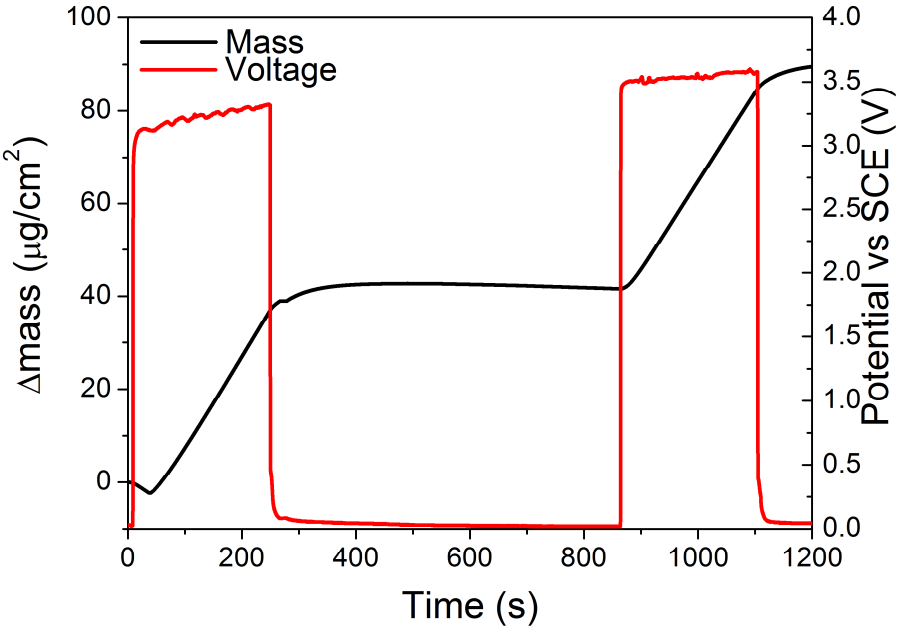

Figure 4: EQCM plot and potential of the electrode vs SCE during two 4 minutes galvanostatic depositions at 0.1 mA/cm^2 separated by a period of 10 minutes during which no current was applied.

After 10 min the current is applied again and, because HKUST-1 crystals are already present on the surface, the deposition continues immediately without a lag-time needed to reach the critical nucleation threshold.

Phase 2: Growth of MOF islands

Both for HKUST-1 and Cu-INA it is observed that, after the first nuclei are formed, new crystals tend to nucleate next to them, forming islands of intergrown MOF (Figure 5). This mechanism was previously observed in the synthesis of MIL-100(Fe) where crystals nucleate on top of the already present ones forming thick layers,[8] and in a recent paper on a Zn-based MOF.[7] The tendency to nucleate new MOF crystals adjacent to existing ones, might be related to the fact that the current density around existing crystals is increased due to the resistance for the flow of current through the MOF crystal. Due to this, the current density and hence the local copper concentration increase in the immediate vicinity of existing crystals which, if the critical nucleation threshold is surpassed, will lead to the formation of new nuclei.[16] Moreover, the formation of islands might explain why it is not needed to reach the critical concentration to grow a layer when MOF crystals are already present on the surface, like in the experiment reported in Figure 4.
As already reported for the solvothermal synthesis of HKUST-1,[17] the nucleation during electrochemical synthesis of this MOF is progressive and extends well into the crystal growth phase. Therefore, while in the first seconds the crystals have almost all the same size, after the first minutes of synthesis big (grown) crystals and small just nucleated ones are present in the solvothermal bath. This behavior was also observed in the electrochemical synthesis, as shown in Figure 6: The size distribution of the crystals broadens with time, and the average size increases.

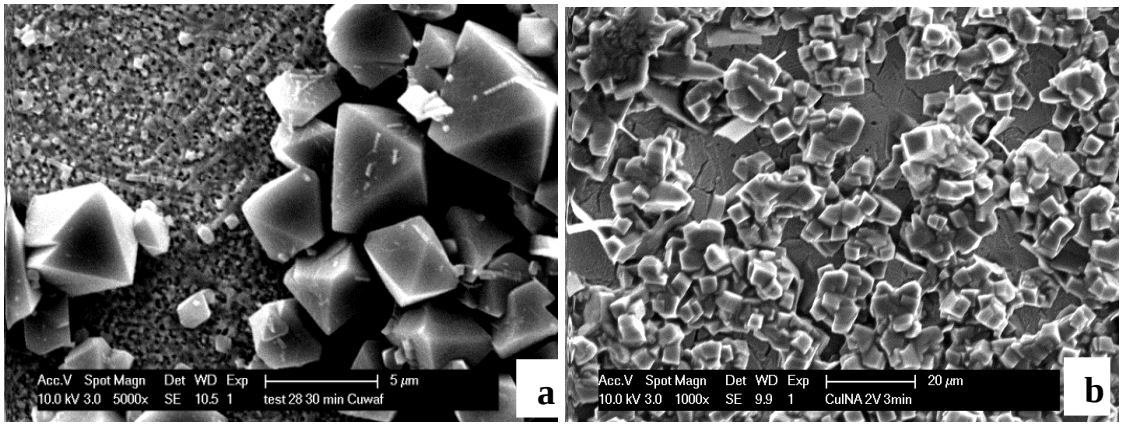

Figure 5: (a) SEM pictures of HKUST-1 deposition after 20 min at 2 V vs counter on a copper-coated wafer. (b) Cu-INA layer synthesised at 2 V vs counter for 3 min.

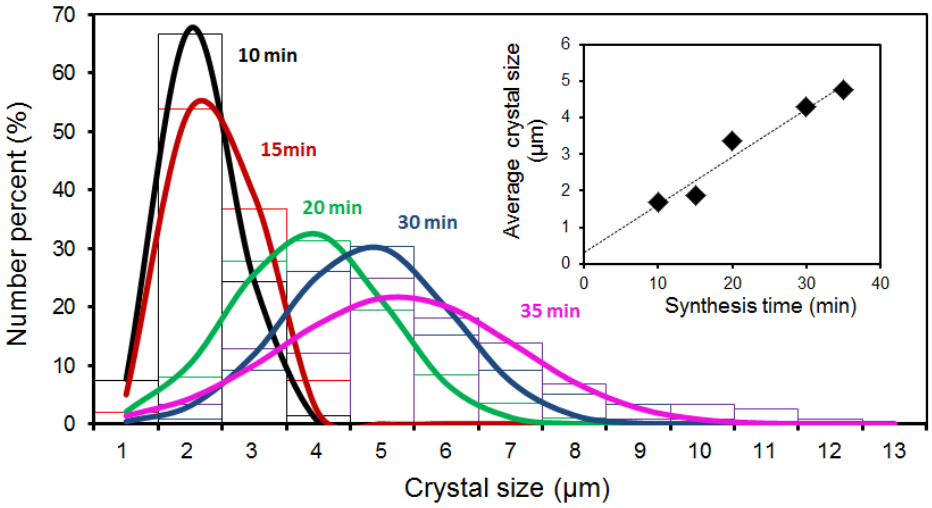

Figure 6: Size distribution as a function of time for HKUST-1 crystals grown potentiostatically at 2.7 V vs. the counter electrode on a copper mesh in an ethanol/water (65:33 vol%) solution at 50 °C.

Phase 3: intergrowth

A very important phase of the deposition is the intergrowth. The crystals keep on nucleating on the surface and in the meantime those already nucleated grow to dimensions of several microns eventually forming a compact layer (Figure 5 and Figure 6). Electrochemically synthesized MOF coatings are therefore self-closing since the growth tends to cover all the metal surface still exposed rather than grow, for example, in a dendritic mode.

Stresses arise in most electrodeposition processes.[18] In the case of MOF electrodeposition the compactness of the intergrown crystals forming the layers is expected to stress compressively the surface. A home-made laser curvature device was built and used to measure the stresses occurring at the surface during electrodeposition. The cantilever used as working electrode for the experiments has a conductive face which was coated with copper, and a non-conductive one which is used to reflect a laser beam. Applying Stoney's formula, it is possible to calculate the stress in the film.

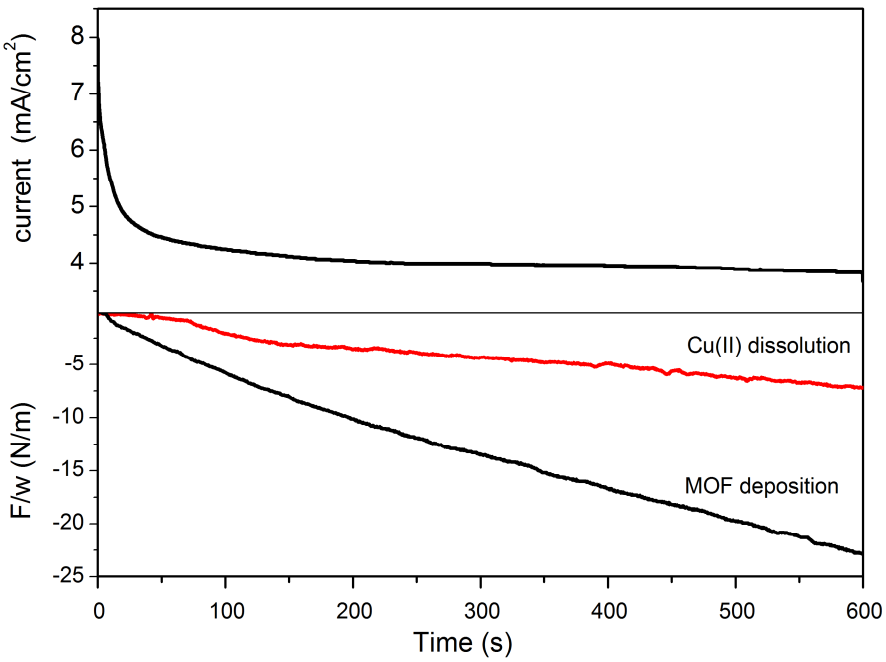

Figure 7: Current and stress measured during potentiostatic MOF deposition (2 V vs counter) in a solution containing 10 g/L MTBS and 10 g/L H_3BTC with a laser curvature set-up, and stress evolution during copper dissolution in a blank solution (without linker) under the same conditions.

Figure 7 shows the stress evolution in the copper film upon deposition of HKUST-1. A compressive stress arises from the first instants when the potential is applied. The compressive stress is partially due to the dissolution of the copper film which contains tensile stress[14, 19] and to the deposition of HKUST-1 crystals. As stated before, a compression stress is in good agreement with the appearance of most MOF layers and HKUST-1 ones in particular: the layers appear to be constituted by continuous films of intergrown crystals with good adhesion to each other, and while buckling of the layers can be observed, cracks have never been reported for this MOF.[11]

The effect of the variation of water to alcohol concentration in the EC synthesis of MOF layers has already been reported.[10] A further investigation shows that changing the organic solvent from ethanol to methanol, DMF, DMSO or ACN has also a pronounced effect on the formation of HKUST-1 layers by electrochemical synthesis. Figure 8 shows SEM pictures of samples synthesized at 50 °C and 2.7 V for 20 min on copper meshes with different solvents, all containing 35 wt.% of water. Mixtures of methanol, ethanol or DMF and water result in relatively large and well defined octahedral crystals. Syntheses run in acetonitrile result in undefined fine particle layers, while DMSO yields a dense layer of small crystals.

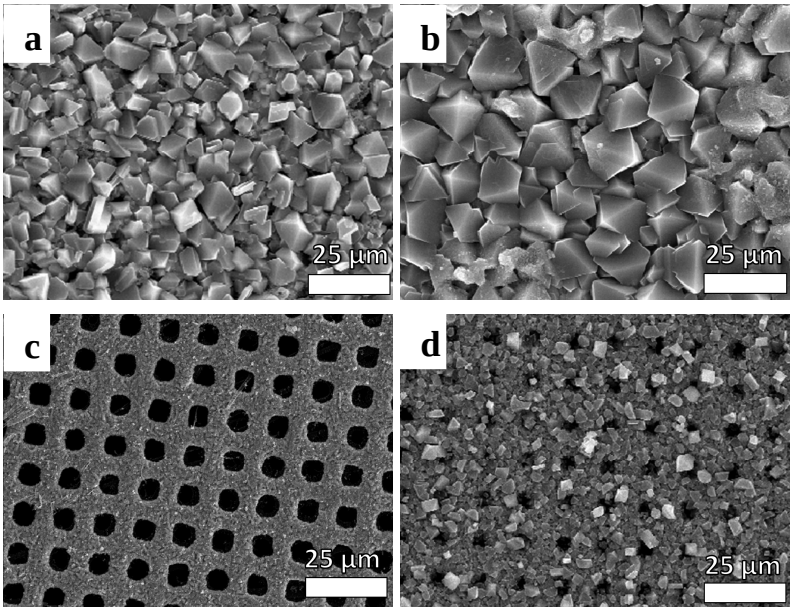

Figure 8: SEM pictures of HKUST-1 layers synthesized on a copper mesh at 2.7 V vs counter for 20 min in solutions containing 16 g/L of BTC in 65 wt% of methanol (a), ethanol (b), acetonitrile (c), and DMF (d) and 35 wt% of water.

XRD analyses proved HKUST-1 to be formed for all the solvent compositions tested, except ACN/water (layers synthesized with this solvent did not show detectable diffraction peaks). Nevertheless, all the solvents yielded layers of a blue compound, and these layers, when tested for the adsorption of methanol, show the two-step profiles typical of HKUST-1. This two-step uptake is related to the structure of HKUST-1, and thus provides a proof of the presence of the right crystalline phase.[20]

As described already, MOF coatings can be synthesized electrochemically as one compact thin layer of intergrown crystals.[5] But if the conditions are favorable[8] or the synthesis is run for longer times,[9] the obtained layers are more than one crystal thick. As schematized in Figure 9, once the substrate is fully covered, further growth of the MOF layer can happen either at the MOF-substrate interface, or at the MOF-solution interface. Taking HKUST-1 as an example, a first approach to understand where the MOF layer grows once the substrate is fully covered is to look at the dimensions of the MOF micropores in comparison to those of the ions and linkers. The distorted octahedron characteristic of solvated copper(II) ions generated at the anode can pass through the MOF structure, since the hydrated copper(II) ions have a diameter of 0.456 nm,[21] while the pores of HKUST-1 have a size of 0.9 × 0.9 nm.[22] Indeed, the motion of small ions through MOF structures has already been shown in MOF-based batteries[23] and supercapacitors[24] electrodes. Another proof of the motion of metal ions through the MOF layers is the edge effect often observed in the synthesis of MOF layers: when no mask is used in front of the anode, the MOF layer grows only at the edges of the electrode, leaving bare copper in the center. In fact, if the layers were perfectly insulating and solvated ions could not go through them, the growth, from a macroscopic point of view, would start from the edges of the anode (where the current density is highest) and continue toward the center, eventually covering the whole surface. On the other hand, BTC^{3-} molecules are expected to be too large to go inside the pores since the minimum calculated diameter of the planar molecule is 2.1 nm,[25] twice the dimensions of HKUST-1 pores.

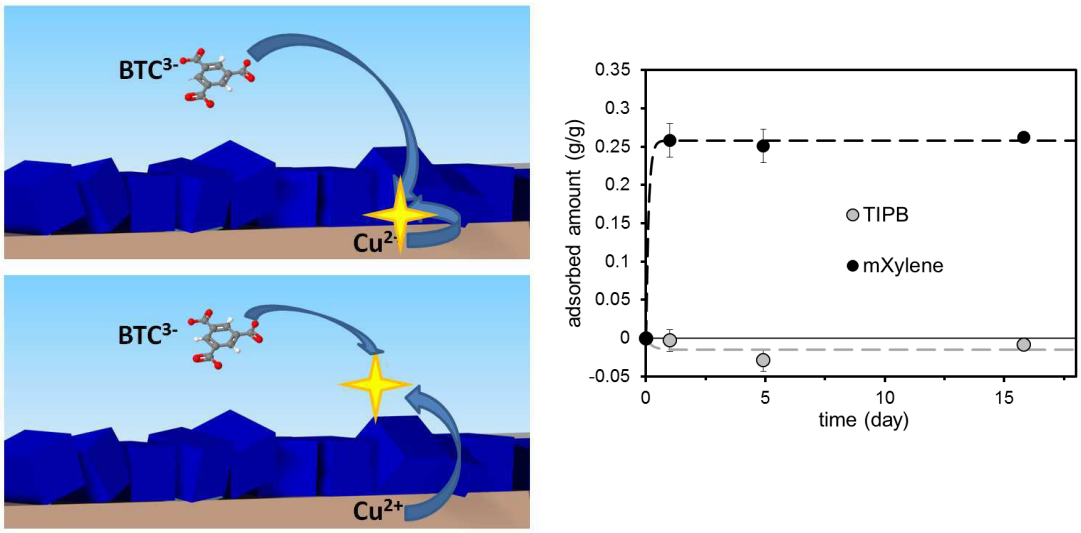

Figure 9: Left: scheme of the two possible mechanisms of MOF growth: from the bottom of the already existing film (top), or from the top of the existing film (bottom). Right: adsorption behavior of HKUST-1 in m-xylene and tetraisopropylbenzene atmospheres.

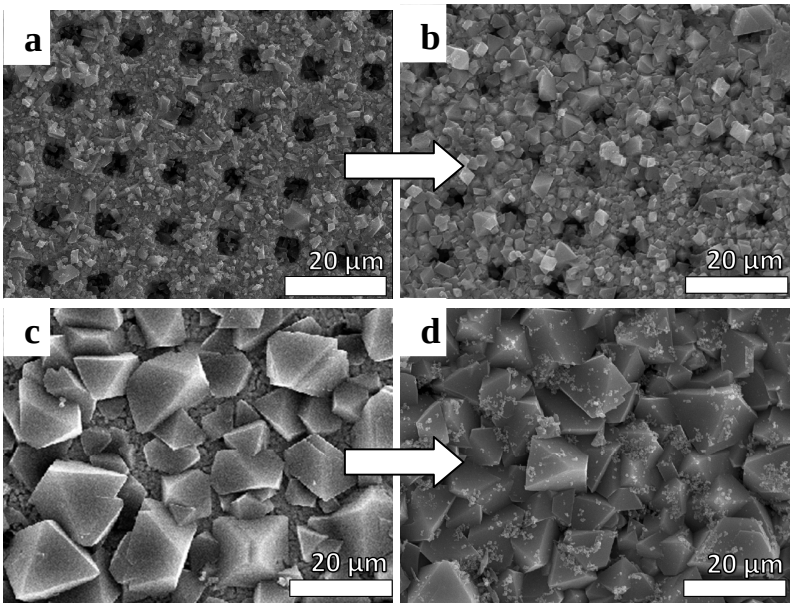

Figure 10: (TOP) HKUST-1 synthesized at 2.7 V vs counter for 20 min on a copper mesh using first a DMSO/MeOH (35:65 wt%) mixture (a) and then a water/MeOH (35:65 wt%) mixture in a second step (b). (BOTTOM) HKUST-1 synthesized at 2.7 V vs counter for 20 min using a water/MeOH (35:65 wt%) mixture and in a second step a DMSO/MeOH (35:65 wt%) mixture.

The adsorptions of m-xylene and 1,3,5-tris(propan-2-yl)benzene in HKUST-1, shown in Figure 9, corroborate the expectations based on the size of the ions since m-xylene which is smaller than BTC can be absorbed by the MOF while the chemically similar but larger 1,3,5-tris(propan-2-yl)benzene is not adsorbed even after several days.
Further indications that the MOF layer grows at the MOF-electrolyte interface were obtained by using different solvents for the synthesis of the MOF, since different solvents lead to MOFs with different crystal size. For example, HKUST-1 layers synthesized in DMSO/methanol mixtures are composed of crystals sizably smaller than those

synthesized in water/methanol. If a substrate is first subjected to electrodeposition and in one solution, and then in another, the final morphology reflects the two treatments; in particular the crystals expected from the last used of the two electrolytes used are found preferentially on top of those expected by the first solvents (Figure 10).

These tests give strong indications that MOF growth occurs at the MOF-electrolyte interface but are not conclusive. It was therefore decided to run a set of experiments using modified linkers to have elemental markers in the MOF structure. HKUST-1, the archetypical MOF normally used for the electrochemical synthesis, is based on copper ions and trimesic acid, and the modification of this linker to add elemental markers is very challenging. Therefore, it was decided to conduct this investigation with another MOF: copper isonicotinate (Cu-INA). In contrast with trimesic acid, isonicotinic acid can be purchased with fluorine and chlorine as substituents (Figure 11). These two halogen atoms are small enough to not sterically alter the framework and can be detected by EDS. The objective of the new set of experiments, similarly to what is described above, was to synthesize two layers sequentially, in order to see where the new layer grows, thanks to the fluorine and chlorine signals. The electrochemical synthesis of Cu-INA layers was already reported,[11] but it is the first time that the synthesis of the substituted versions of this MOF is reported.

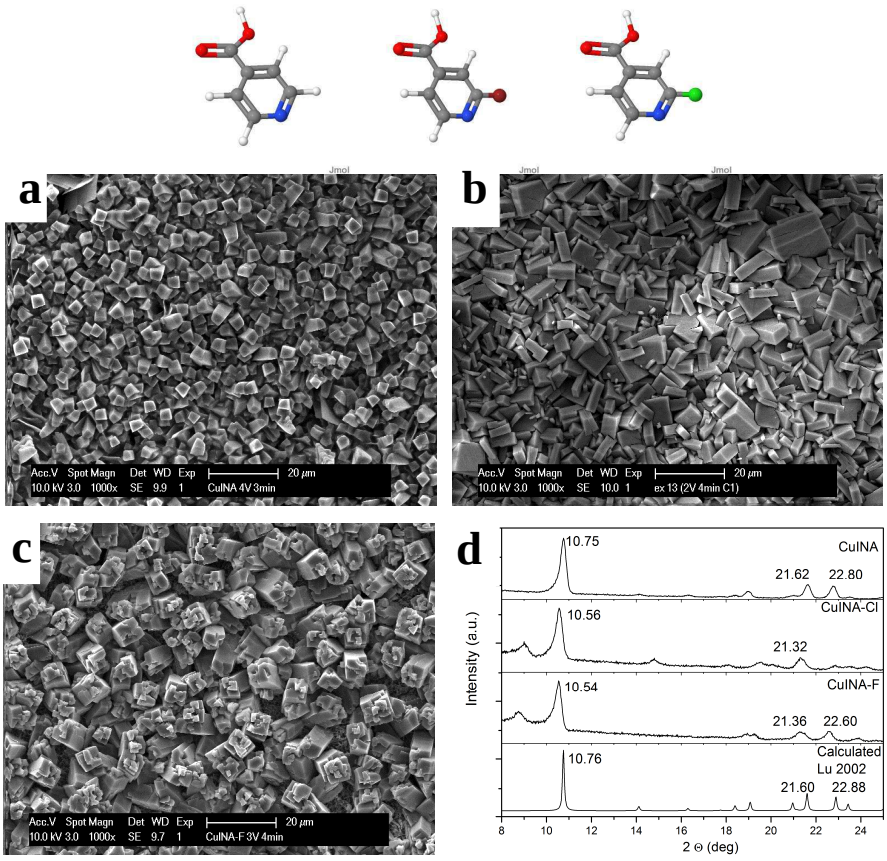

Figure 11: Linker molecules: HINA, HINA(Cl) and HINA(F). SEM pictures of Cu-INA (a), Cu-INA(Cl) (b) and Cu-INA(F) (c) layers. (d) Comparison between the XRD patterns of Cu-INA, Cu-INA(Cl), Cu-INA(F), and the calculated pattern from Lu *et al.*[26]

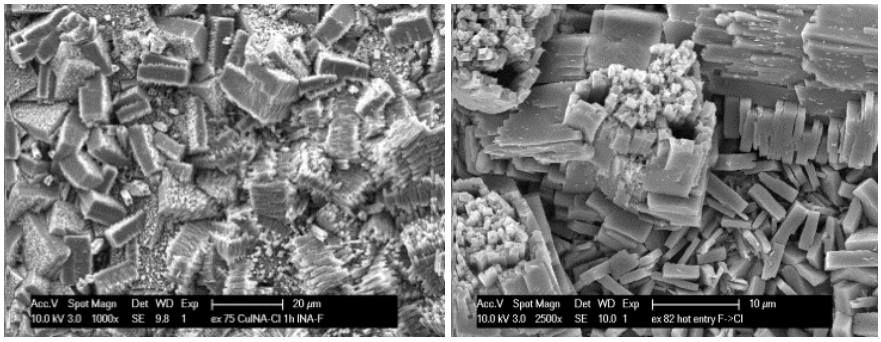

Figure 12: SEM pictures of a Cu-INA(Cl) sample synthesized for 4 min and then left in INA(F) solution for 1 h without applying any voltage, and a Cu-INA(F) sample synthesized for 4 min in INA(F) and 4 min in INA(Cl).

The synthesis of Cu-INA(X) (with X = Cl or F) was achieved by modifying the electrolyte composition, the applied potential, and the synthesis time. In comparison to Cu-INA which can be synthesized as a pure phase, in none of the conditions tested it was possible to avoid the deposition of a needle-shaped pre-phase. This pre-phase can be synthesized pure if low potentials are kept, while at higher potentials the cubic phase reported also for Cu-INA is present. Unfortunately at too high potentials, detachment of the layers is observed. The shape of the crystals changes with the different linkers: while Cu-INA looks like truncated pyramids, Cu-INA(Cl) crystals resemble plates, and Cu-INA(F) are more like cubes (Figure 11). All the samples are undistinguishable from the XRD patterns, except for the fact that the layers made by the substituted versions show a small peak shift to lower angles and also the peak of the pre-phase. This pre-phase crystalline and has already been indexed by Tran *et al.* in the P21/n space group,[27] while the more studied and already synthesized phase is also monoclinic but from the CC group.[26]

In order to study the formation of multilayer coatings, the first formed layer must be stable in the solution used. Post-synthetic linker exchange has been reported by several authors,[28, 29] and is even more likely in this experiment as the linkers used are very similar and the second layer is grown in synthesis conditions similar to those of the first one. We observed that with Cu-INA(X) layers, the linker substitution occurs even if no current is applied, and the morphology of the layers changes towards shapes more similar to those expected for the alternative linker. Figure 12 shows the surface morphology of two Cu-INA(X) layers synthesized and then exposed to a solution of the other halogenated isonicotinate, with and without current imposed. In both cases the top layer undergoes major changes upon exposure to the new linker. When the layer is just left in solution, the crystals only change their shape, while when current is applied the new phase grows from the existing one. This is very evident in Figure 12, where the plate shaped crystals typical of Cu-INA(Cl) grow perpendicularly on top of the Cu-INA(F) cubes.

The deposition of a coating made by a sequence of two layers of Cu-INA(X) was achieved by growing a thick and compact first layer, followed by the deposition of the second, exposing the MOF layer for as little time as possible to the solution with the new linker. The cross-sections of the resulting layers have been analyzed by NanoSEM and EDS (Figure 13). Already from the morphological analysis of the crystals and their positions, it might be speculated that the growth of new crystals happens on top of the existing one, but the elemental mapping shows unequivocally that the new MOF grows on top of the old MOF.

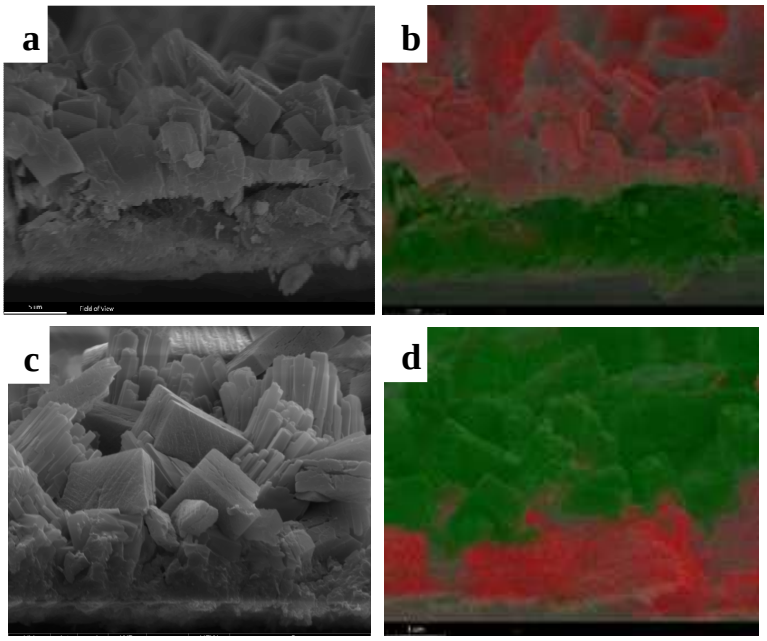

Figure 13: (top) NanoSEM picture (cross-section) without (a) and with (b) elemental contrast of a Cu-INA(F) layer synthesized on a plate with already Cu-INA(Cl) on it. (bottom) NanoSEM picture (cross-section) without (c) and with (d) elemental contrast of a Cu-INA(Cl) layer synthesized on a plate with already Cu-INA(F) on it. The green signal is due to chlorine and the red to fluorine.

A net division in concentration of the halogen elements is observed: chlorine is found at the bottom when Cu-INA(Cl) is synthesized first, and on the top when Cu-INA(Cl) is synthesized last, and the analogous behavior is observed for fluorine. Therefore, it can be stated that the first layer synthesized is found on the bottom of the film and the second on the top and hence MOF layers grow at the MOF-electrolyte interface by the diffusion of copper through the MOF layer.

Phase 4: detachment

During the last phase, crystals detach from the surface and expose empty spots of bare metal. This phase of the deposition has to be avoided if a high quality deposition is targeted. The reason behind the detachment is the mechanism of the MOF growth elucidated above. As demonstrated when using the fluorine and chlorine substituted nicotinic acid, the copper ions migrate through the MOF layer to react at the MOF-solution interface. This implies that the copper substrate below the MOF layer dissolves due to the electrochemical formation of copper ions creating voids below the MOF layer. These voids eventually lead to the buckling of the MOF layer (due to the compressive stresses shown previously) and detachment of single crystals or, more often, of large coating areas.
Moreover, it is observed that during the electrochemical MOF synthesis, the copper substrate does not dissolve uniformly, but preferentially dissolves at certain locations. These preferential sites do not correspond to the space between MOF crystals, but possibly to the grain boundaries of the substrate (Figure 14d).

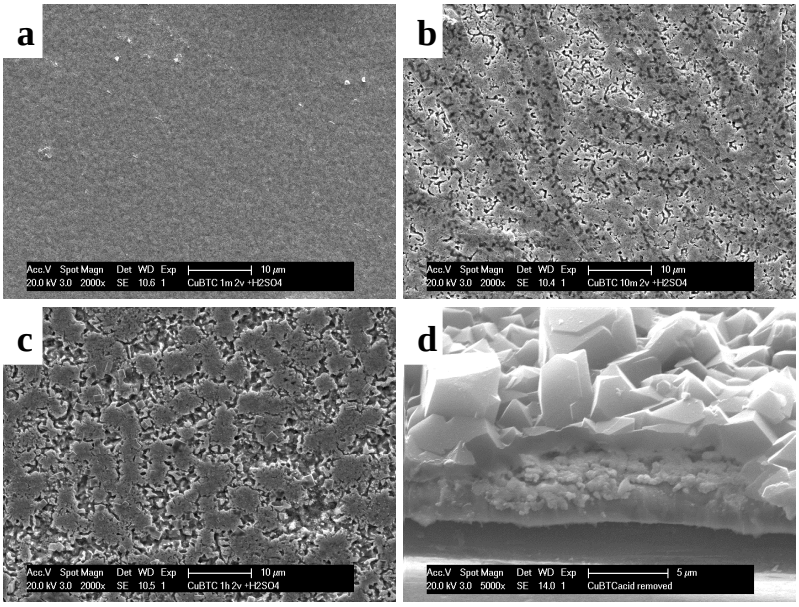

Figure 14: SEM pictures of layers (synthesized at 2 V vs Ag after 1 (a), 10 (b) , and 60 (c) min on copper-coated silicon wafers) dipped in diluted H_2SO_4 solution to remove the MOF crystals. The images show the evolution of the copper substrate underneath. On the bottom the same sample synthesized for 60 s is viewed from the top (c) and with part of the coating not dissolved by the acid, at 75° angle with the normal (d).

Conclusions

In this paper a mechanism has been proposed to explain the electrodeposition process of Metal-Organic Frameworks (MOFs). The deposition is divided into four phases: (I) initial nucleation, (II) growth of MOF islands, (III) intergrowth, and (IIII) crystal detachment. When an electric potential is applied, a lag time is needed before the electrodeposition of MOF on a bare surface starts. The duration of this lag time depends on the applied current and arises from the time that is needed to reach the critical ion concentration threshold for nucleating the new MOF phase. On the other hand, when MOF crystals are already present on the surface, the electrodeposition starts immediately. The growth of MOF layers happens at the MOF-solution interface, meaning that copper ions are dissolved at the metal-MOF interface, migrate through the MOF layer and react with the linker from the solution. This leads to the creation of voids at the substrate-MOF interface that eventually lead to the buckling of the brittle MOF layers and detachment due to undercut.

Acknowledgments

The authors would like to acknowledge Tom Van der Donck (Hercules 3 ZW09-09 project) for the NanoSEM pictures and professor B. W. Sheldon for the interesting discussion and the suggestions on the stress evolution part. The authors thank IWT for the support in the SBO project MOFShape.

References

1. S. S. Y. Chui, S. M.-F. Lo, J. P. H. Charmant, A. G. Orpen and I. D. Williams, *Science*, 1999, **283**, 1148-1150.
2. N. Stock and S. Biswas, *Chem. Rev.*, 2011, **112**, 933-969.
3. H. Furukawa, K. E. Cordova, M. O'Keeffe and O. M. Yaghi, *Science*, 2013, **341**.
4. U. Mueller, 2007, **US Patent 2007/0227898 A1**.
5. R. Ameloot, L. Stappers, J. Fransaer, L. Alaerts, B. F. Sels and D. E. De Vos, *Chem. Mater.*, 2009, **21**, 2580-2582.
6. A. Betard and R. A. Fischer, *Chem. Rev.*, 2012, **112**, 1055-1083.
7. K.-Y. Cheng, J.-C. Wang, C.-Y. Lin, W.-R. Lin, Y.-A. Chen, F.-J. Tsai, Y.-C. Chuang, G.-Y. Lin, C.-W. Ni, Y.-T. Zeng and M.-L. Ho, *Dalton Trans.*, 2014, **43**, 6536-6547.
8. N. Campagnol, T. Van Assche, T. Boudewijns , J. F. M. Denayer, K. Binnemans, D. E. De Vos and J. Fransaer, *J. Mater. Chem. A*, 2013, **1**, 5827 - 5830.
9. T. R. C. Van Assche and J. F. M. Denayer, *Chem. Eng. Sci.*, 2013, **95**, 65-72.
10. T. R. C. Van Assche, G. Desmet, R. Ameloot, D. E. De Vos, H. Terryn and J. F. M. Denayer, *Micropor. Mesopor. Mat.*, 2012, **158**, 209-213.
11. B. Van de Voorde, R. Ameloot, I. Stassen, M. Everaert, D. De Vos and J.-C. Tan, *J. Mater. Chem. C*, 2013, **1**, 7716-7724.
12. A. Martinez Joaristi, J. Juan-Alcañiz, P. Serra-Crespo, F. Kapteijn and J. Gascon, *Cryst. Growth Des.*, 2012, **12**, 3489-3498.
13. J. Newman, *J. Electrochem. Soc.*, 1966, **113**, 501 - 502.
14. O. E. Kongstein, U. Bertocci and G. R. Stafford, *J. Electrochem. Soc.*, 2005, **152**, C116-C123.
15. K. M. Ogle, C. Gabrielli, M. Keddam and M. Perrot, *J. Electrochem. Soc.*, 1994, **141**, 2655-2658.
16. J. Fransaer and J. R. Roos, *J. Heat Transf.*, 1992, **114**, 317-325.
17. F. Millange, R. El Osta, M. E. Medina and R. I. Walton, *CrystEngComm*, 2011, **13**, 103-108.
18. F. Czerwinski, *J. Electrochem. Soc.*, 1996, **143**, 3327-3332.
19. S. Ahmed, T. T. Ahmed, M. O'Grady, S. Nakahara and D. N. Buckley, *J. Appl. Phys.*, 2008, **103**, 103 - 115.
20. T. R. C. Van Assche, T. Duerinck, J. J. Gutiérrez Sevillano, S. Calero, G. V. Baron and J. F. M. Denayer, *J. Phys. Chem. C*, 2013, **117**, 18100-18111.
21. I. Persson, *Pure Appl. Chem.*, 2010, **82**, 1901-1917.
22. C. Prestipino, L. Regli, J. G. Vitillo, F. Bonino, A. Damin, C. Lamberti, A. Zecchina, P. L. Solari, K. O. Kongshaug and S. Bordiga, *Chem. Mater.*, 2006, **18**, 1337-1346.
23. R. Demir-Cakan, M. Morcrette, F. Nouar, C. Davoisne, T. Devic, D. Gonbeau, R. Dominko, C. Serre, G. Férey and J. M. Tarascon, *J. Am. Chem. Soc.*, 2011, **133**, 16154-16160.
24. N. Campagnol, R. Romero-Vara, W. Deleu, L. Stappers, K. Binnemans, D. E. De Vos and J. Fransaer, *ChemElectroChem*, 2014, -.
25. calculated with *chemicalize.org*.
26. J. Y. Lu and A. M. Babb, *Chem. Comm.*, 2002, 1340-1341.
27. D. T. Tran , X. Fan, D. P. Brennan, P. Y. Zavalij and S. R. Oliver, *Inorg. Chem.*, 2005, **44**, 6192-6196.

28. O. Karagiaridi, W. Bury, J. E. Mondloch, J. T. Hupp and O. K. Farha, *Angew. Chem. Int. Ed.*, 2014, **53**, 4530-4540.
29. J. G. Nguyen and S. M. Cohen, *J. Am. Chem. Soc.*, 2010, **132**, 4560-4561.